CLASSIFICATION AND RADIO SCIENCE MODELING OF RADAR METEOR ECHOES

Jennifer Cross* and John D. Mathews†

Department of Electrical Engineering
The Pennsylvania State University
University Park, PA 16802

*Undergraduate student in
Electrical and Computer Engineering
Franklin W. Olin College of Engineering
Needham, MA 02492

ABSTRACT

This paper documents the results of two phases of research: first, the classification of micrometeor events into a collection of specimen events; and second, the creation of a simplified radio science model able to explain a large number of these specimen events. This model is especially equipped to further investigate the existence of fragmentation within approximately 17,000 micrometeor events recorded by the Arecibo Observatory located in Puerto Rico. Our analysis of these events identified many specimens showing the cyclical constructive and destructive interference which we found to be consistent with a micrometeor consisting of a few fragments. This simple interference is indicated by regular interference cycling between multiple pulses (pulse-to-pulse) and within single radar pulses (intrapulse). Our model demonstrates these interference patterns can be completely explained and represented by a model which focuses on radio interference alone and simplifies meteor ablation, plasma physics, the antenna gain pattern and the radar equation into a singular variable. We found that while it is a relatively straight forward process to use the model to emulate these simple interference specimens, the majority of specimen events have more complex interference resulting most likely from a

†Faculty Mentor

larger number of fragments. This compound interference, while theoretically possible to generate using the current model, is too complicated to accurately emulate a specific specimen with our current brute force methods given the large number of interrelated variables.

Further development of this model could include the incorporation of factors such as antenna gain that were previously neglected in order to provide more accurate emulations which allow greater flexibility in the represented meteor science. Other model improvements such as the creation of automated emulation generation algorithms could permit the emulation of specimen with complex interference. This research provided a strong foundation for future modeling attempts while also identifying a set of specimen events which will serve as a tool for highlighting the strengths and weaknesses of current and future models.

INTRODUCTION

Every year, a huge quantity of material from space enters earth's atmosphere. The objects that make up this material flux are known as meteoroids and range in size from a micron or less (known as micrometeoroids) to larger specimens that are multiple meters in diameter. While passing through the earth's atmosphere at high velocities, these objects heat and experience a loss of material through evaporation in a process known as ablation. Meteoroids larger than a millimeter produce visible streaks of light commonly referred to as "shooting stars" that are more specifically known as meteors. The vast majority of these meteoroids disintegrate entirely before reaching the earth's surface leaving unknown quantities of matter and energy in the atmosphere.[1] Those meteoroids that are large or slow enough to be able to pass through the atmosphere to impact the earth's surface are designated meteorites, which are a source of interest for many enthusiasts and scientists who seek to learn more about meteor and planetary science.

Advancing the current state of meteor science requires us to answer many questions about the impacts that this incoming material has on the planet earth. Through the further investigation of meteoroids and meteors, we are able to gain understanding about the amount and composition of material that is deposited in the earth's atmosphere by the ablation of these objects.[1] The effect of the energy generated by the movement of the meteors also has unknown effects. Encounters with these objects may also impact orbiting space devices which do not benefit from the protection of the atmosphere and thus have potential to sustain damage from even the smallest of these meteoroids.

While only large meteors are visible to the naked eye, the introduction of RADAR brought with it the ability to observe far smaller meteors. RADAR which originally served as an acronym for "radio detecting and ranging" is used to describe any of a number of devices which utilize certain principles to collect range data about target objects. Each radar has a transmitter which produces an electromagnetic signal which travels through space to a distant object. The target reflects

some amount of this signal, the echo, and it is retransmitted in all directions. Some of this reflected signal is returned towards the radar's receiver. Once received, the echo can be used to calculate a wide variety of properties of the target, such as it's distance, radial velocity and reflectivity.[2]

As meteoroids undergo ablation through collisional interaction with the atmosphere, they reach extremely high temperatures as particles, usually atoms such as aluminum or iron, are removed from the meteoroid. These ablated particles ionize directly behind the meteoroid forming a "blob" of plasma. While the very small micrometeoroids would be invisible to the radar, this"blob" of plasma serves as a larger target to reflect a stronger echo back towards the radar receiver. The echo that is returned is called the "head echo" of the meteor.[3] These head echoes permit the measurement of the meteor's altitude, velocity, deceleration and very importantly for the focus of this paper, fragmentation. Another type of echo, known as a "anomalous trail echo" (or Range-Spread Trail-Echo) results from the radar's signal reflecting off of the trail of plasma left behind along the path of the meteoroid. These trail and head echoes of micrometeorites are most commonly observed utilizing high power, large aperture (HPLA) radars which transmit very strong signals and have very sensitive receivers.[4]

While effort and focus is being invested in understanding and modeling the plasma physics and meteor science which produce these meteor echoes (as shown in Dyrud and Janches[1]), much of what is observed may also explained and interpreted using radio science and simple radio science models. Such effort towards the characterization and classification of data recorded using HPLA radar helps to better understand the meteor phenomena that it represents. This allows greater accuracy in estimating the properties of meteors and meteoroids that are observed using HPLA radars.

In this paper, we will seek to further classify and explore the effects of fragmentation and the related radio science phenomena. Following this analysis, we will introduce models to further the verification of these classification schemes. This will provide a radio science basis for interpreting different phenomena such as signal interference. In addition, the models permit the estimation of micrometeoroid parameters such as the differential speed between fragments and meteoroids.

OBSERVATIONAL SETUP

The data we analyze in this paper were collected at the Arecibo Observatory, located in Puerto Rico. As a HPLA radar telescope, the Arecibo Observatory (AO) collects regular data on micrometeor events.[3] The data analyzed in this paper collected on June 2, 2008 and June 3, 2008 yielded approximately 10,000 and 7,000 observed micrometeor events, respectively. The data associated with these events were identified utilizing an event detection signal processing method developed by Mathews *et al.*[5] and Briczinski *et al.*[6] The data were then visually inspected as range time intensity (RTI) plots in order to perform case-by-case classification of

Figure 1: Image of Arecibo Observatory, Puerto Rico. Photograph courtesy of the NAIC - Arecibo Observatory, a facility of the NSF

different types of meteor and radio phenomena observed.

The events were simultaneously recorded using VHF and UHF radar frequencies. The UHF radar utilizes a 430 MHz signal with a very narrow (1/6°), sensitive receiver antenna beam possessing side lobes as made visible in Figure 2 and allowing it to pick-up echoes from very small, weak micrometeoroids. For the data associated with this paper, the UHF radar was set to send 20 microsecond pulses with an interpulse period of 1 millisecond. The VHF radar utilizes a 46.8 MHz signal with a wider and less sensitive receiver antenna beam (1.2°) that is co-axial with the 430 MHz antenna. This wider antenna geometry allows it to generally pick-up only stronger echoes but each remains visible in the wider beam for a longer period of time.[4] The VHF radar was set to send 10 microsecond pulses with an interpulse period of 1 millisecond. These simultaneously occurring sets of data, utilizing two radar frequencies, allowed us to have alternative perspectives on each meteor event. This yields additional information about the radio science phenomena and provides greater insight into the observed physical events than the data from either radar taken individually.

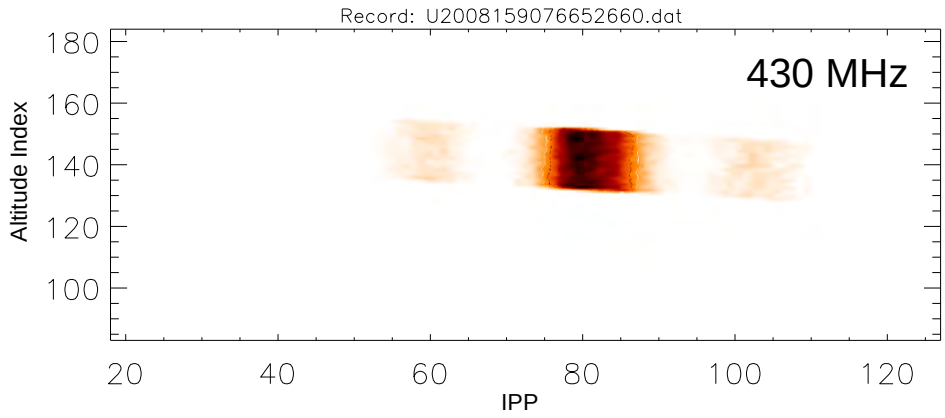

Figure 2: An example of an RTI (range-time-intensity) plot of a meteor head-echo traveling across the Arecibo Observatories UHF antenna gain pattern. In the figure, the echo from first side-lobes are visible surrounding the echo observed with the principal radar beam. The altitude index indicates 150 m changes in altitude in the 80 to 140 km region.

RESULTS AND DISCUSSION

Fragmentation Radio Science

The radar UHF and VHF signals, 430 MHz and 46.8 MHz respectively, are each, as electromagnetic signals, capable of undergoing constructive and destructive interference when two signals of similar frequencies are received simultaneously. Occurring in much the same way that the standard physics "double-slit experiment" demonstration highlights interference created by two visible light sources of similar frequencies, radar scattering targets act as the sources of the echo signals. The light intensity of the double slit at a certain spatial location is then analogous to the echo that is measured by the radar receiver. A single radar scatterer will consistently return an echo of certain power.

The introduction of a second scatterer creates the potential for the existence of signal interference. If the distance between the sources is held constant, the signals received will arrive with a constant phase difference resulting in a certain amount of constructive or destructive interference. However, in order to maintain that constant interference, the radar targets from a fragmented micrometeor must travel at precisely the same velocity towards the receiver. More frequently, as the targets separate or converge, the signal power at the receiver will vary with the cyclical transitions between constructive and destructive interference.

If the targets were simple signal sources, a complete cycle from peak interference to peak interference would occur as the distance between sources increased or

decreased by one wavelength. However since the signals reflecting from the scattering targets are required to travel twice the distance from the radar, as first a pulse then an echo, the effective distance difference between targets is doubled. This means that a complete cycle of interference happens when the distance between the scattering targets increases or decreases by just half a wavelength.

Example Case of Fragment Interference

In Figure 3, the head-echo in the RTI plot is seen clearly in the first 79 pulses at VHF frequency. At 80 pulses, or 80 milliseconds after the initial recording of the event, some meteor science event (which will not be investigated by this paper) occurs. The result appears to be an anomalous trail-echo (based on it's maintained altitude) in addition to the original head-echo which continues descending.

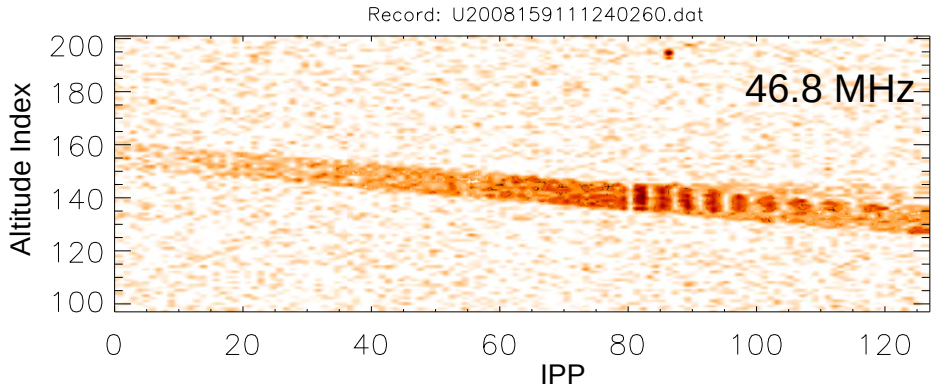

Figure 3: A VHF RTI plot showing initially a single head-echo. At IPP 80, a trail-echo appears which remains at the altitude where it was produced. The head-echo continues descending which results in some pulse-to-pulse interference, seen as the on-off modulation of the full return, between the head-echo and trail-echo.

While these signals are received simultaneously, there is visible pulse-to-pulse fading and strengthening between the two echoes. It is highly likely that this pulse-to-pulse cycling is due to the previously discussed interference, as the radio science model (to be discussed later) to recreate such an interaction is both simple and conceivably possible. As the distance between the stationary trail scatterer and the descending head-echo scatterer increases, the combined signals pass through periods of constructive and destructive interference. Interestingly, the period of these cycles noticeably increases during the observation which is indicative of a reduction in the difference between the scatterers' velocities through either the deceleration of the head-echo scatterer or an (unlikely) acceleration of the trail-echo scatterer. This radio science explanation is further augmented by modeling later in this paper.

Collection of Fundamental Interference Observations

A primary product of the research reported here, was an expansive collection of observed meteor events that were selected from the approximately 17,000 meteor events which were recorded at Arecibo Observatory over the course of two days. The selected meteor events serve as specimens that may be used to further highlight the strengths and flaws in existing and future models of meteor science, plasma physics and radio science in their abilities to explain the different specimens.

Many of the event specimens present very regular cyclical power strengthening and weakening that is consistent with the suggested radio science product of meteoroid fragmentation. In particular, the specimen plots shown in Figure 4 are representive of some of the strongest support for the fragmentation model which is capable of generating such results with the existence of two simply modeled moving point targets. The results of these models will be developed in a later section.

The specimen events were each collected in both the UHF and VHF radar results. While it is rare, likely due to reasons explained by Mathews,[4] a number of specimens exhibit the regular cyclical interference at both frequencies such as those shown in Figure 5. These models further support the radio science models which are able to easily explain the interference cycle period difference when the wavelength differences short wavelength UHF and long wavelength VHF is considered.

Basic Radio Science Model

In order to better explore, experiment and emulate events collected with the radar systems, we generated a model which incorporates as few features as are required to adequately explore the radio science events which are most often seen within the data.

The first assumption that we chose to make for consistency was to assume that all modeled events will be contained in the main antenna beam at both frequencies and move vertically and not horizontally. This allows us to neglect the variations of antenna gain and also reduces the model from the three-dimensional space to a one dimensional model along the major radar axis. For the exploration in this model, we also chose to simplify the model by summarizing the following power equation to a single constant,

$$P_R(meteor) = \frac{P_T L \lambda^2 G^2}{(4\pi)^3 r^4} \sigma_{meteor} \tag{1}$$

where P_R is the power received, P_T is the transmitter power, L is the transmitter system loss coefficient, λ is the signal wavelength, G is the antenna gain, r is the range to the target and σ_{meteor} is the scattering cross-section of the target.[4]

This choice stems from the model's focus on the radio science observations, eliminating the need to immediately consider the effects of antenna gain, the scattering cross-section or the transmitter power which will be held as a constant. Creating this relative power constant also removes the signal power's dependency on the scatterer's distance from the radar. While less than ideal, this approach lim-

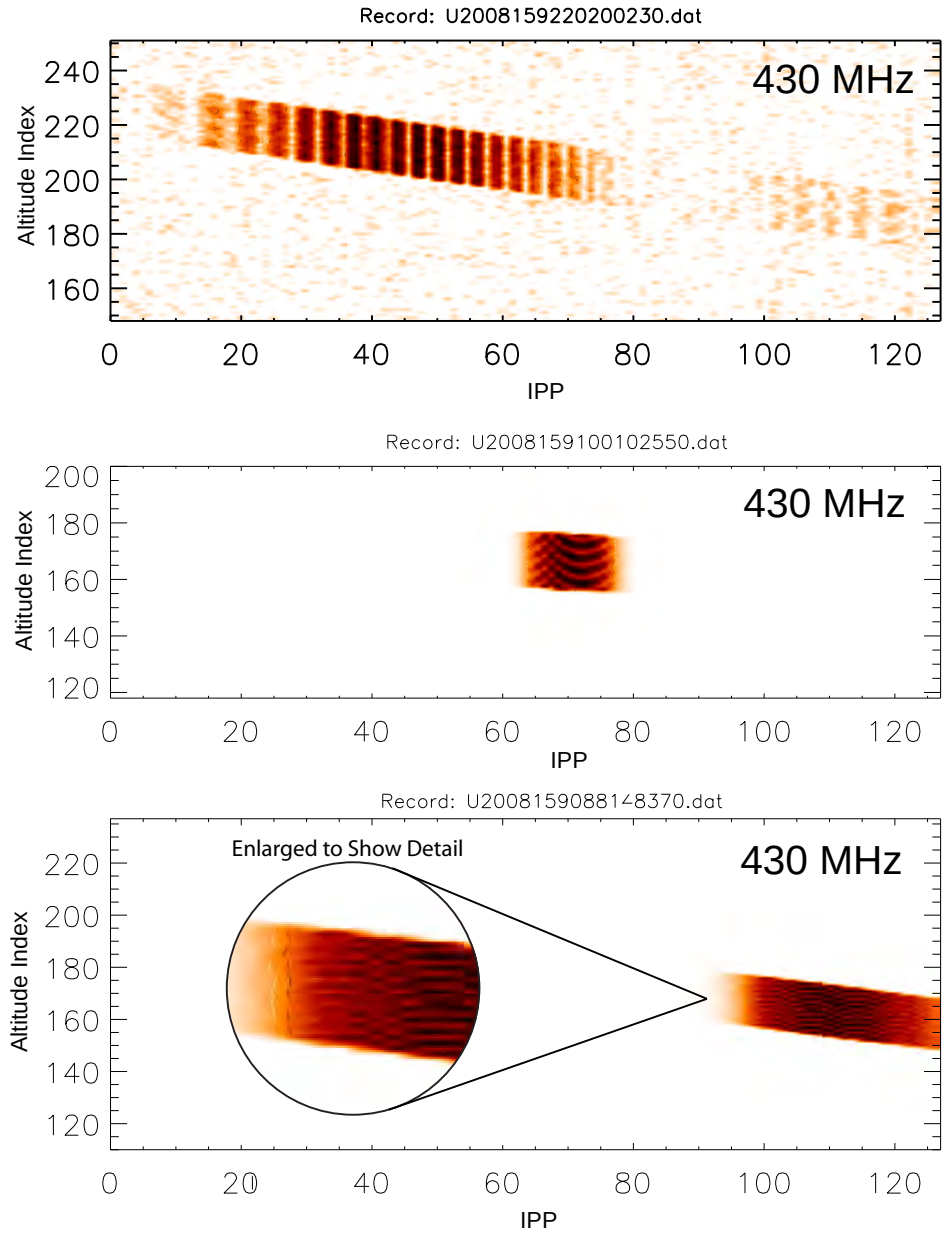

Figure 4: Three UHF RTI plots exhibiting simple interference due to a small number of fragments. Top - The pulse-to-pulse interference cycling results from a velocity difference which is approximately one half wavelength per 4 milliseconds, with much longer period fading likely caused by antenna gain. Middle - Cyclical fading internal to a single pulse indicative of a rapid velocity difference between two fragments which is approximately one half wavelength per 4 microseconds. Bottom - Very fine internal pulse structure indicating a very large velocity difference between fragments, approximately one half wavelength per microsecond.

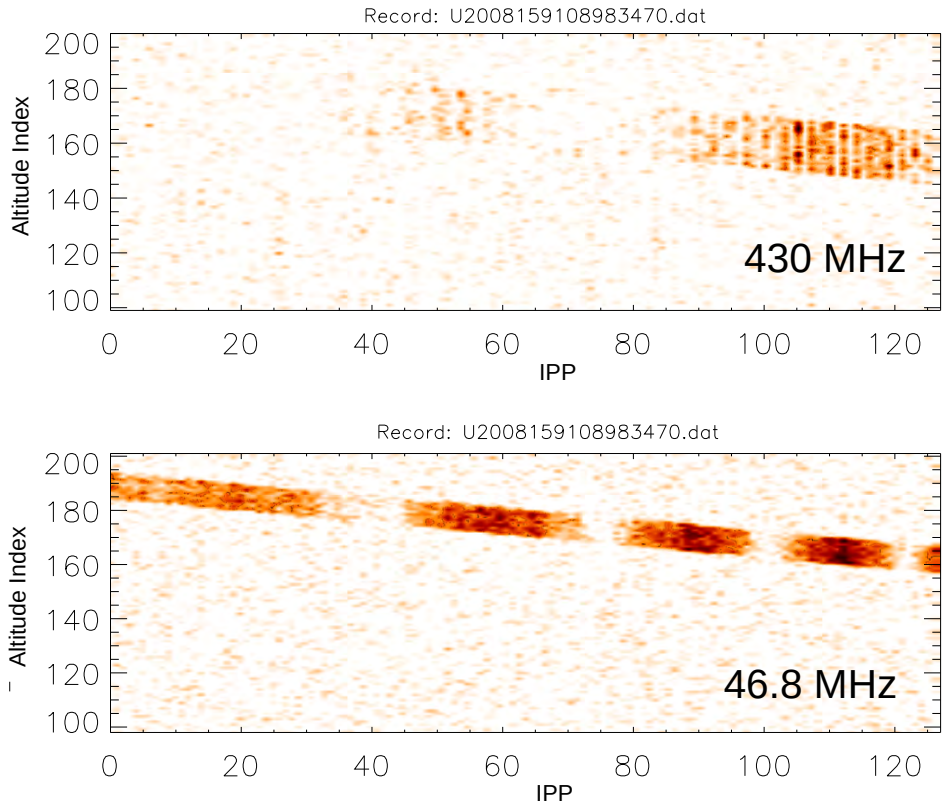

Figure 5: A pair of RTI plots, UHF (top) and VHF (bottom), resulting from the same meteor event. The UHF plot possesses regular quick pulse-to-pulse cycling while the VHF plot has a much slower pulse-to-pulse cycling period reflecting the longer VHF wavelength. Both signals also have some irregular intrapulse structuring either resulting from noise or possibly indicating numerous smaller fragments also contributing to the received signal

its the possible sources of power variations with the model to interference effects alone.

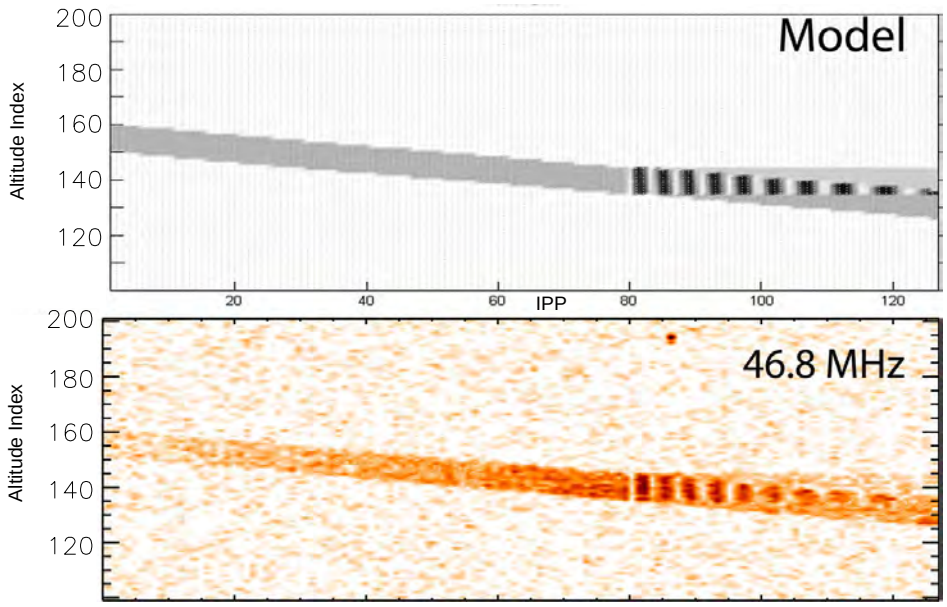

Figure 6: Demonstration of the radio science model showing the model result along side the emulated data from Figure 3

The modeling of the events is broken up into a number of functional blocks within the modeling program. The first feature reflects the movement and modeling of the meteor or plasma blob as radar point targets. Each target (meteoroid head-echo) is represented as a radar point scatterer as was done by Roy *et al.*[7] These target objects contain the physical properties each target, such as a "reflectivity" constant that is representative of variations in the radar backscatter cross-section of the target, velocity of the target along the modeled dimension, acceleration of the target and the target's initial altitude. Additionally, the object may be coded to start and end at arbitrary times in order to compensate for meteor events which would result in the elimination or creation of targets. These objects use the following motion equation based on Roy *et al.*[7] to calculate the the target's range (or altitude):

$$R(t_M) = R_I - v_I * (t_M - t_I) - \frac{a}{2}(t_M - t_I)^2 \tag{2}$$

where $R(t_M)$ is the range of the object at model time t_M, R_I is the initial range of the object when t_M is equal to the starting time of the object t_I, v_I is the initial object velocity of the object (also at time t_I) and a is the acceleration of the object.

The model iterates through individual radar pulses and after each pulse the model discretely increments through time. During each time step, a function representing the ranging functionality of the radar calculates whether or not the emitted

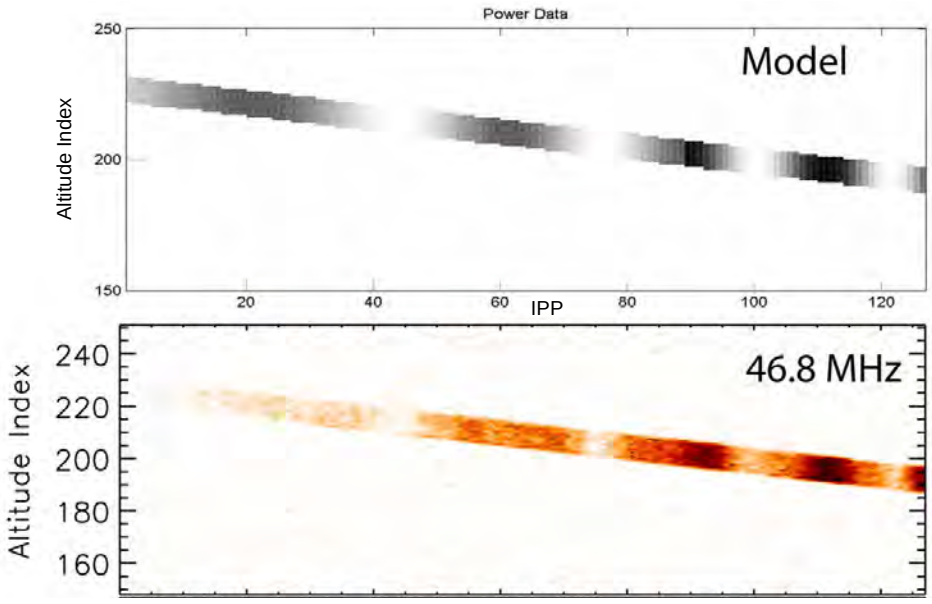

Figure 7: Demonstration of the radio science model, showing the model results along with the emulated data. The emulated data possesses a meteor science phenomena (occurring around pulse 90) which is not accurately explained using the simple radio science model alone.

pulse would have had time to reach each target object and return based on the speed of the signal's propagation and the target's altitude. For echo to have time to return, the model time must fit within the following range:

$$2R_t/C_{radar} < t_M < 2R_t/C_{radar} + t_p \tag{3}$$

where R_t is the range of the target calculated in (2), C_{radar} is the speed of the pulse propagation, t_p is the length of the pulse signal and t_M is the model time.

If there has been adequate time, a function then determines what the baseband signal phase would be given the target's current position (altitude). The complex baseband signal for the target as used in Roy *et al.*[7] is represented as:

$$x_i(t_M) = A_i \exp\left(\frac{i4\pi R(t_M)}{\lambda} t_M\right) \tag{4}$$

where x_i is the baseband signal, A_i is the complex amplitude of the signal, $R(t_M)$ is the range of the target at model time t_M and λ is the radar wavelength.

By accounting for the movement (and resulting decrease in altitude) of the object during the pulse, we are able to automatically account for Doppler shifting of the signal. Adding the signal echo from each object at each discrete delay time permits us to accommodate multiple fragments and allows us to model the phenomena of signal interference from multiple fragments. We then created emulations of

simple event specimens by calculating approximate initial altitudes, velocities, differences in fragment velocities and accelerations based on the recorded data of the specimen. The model parameters were then fine tuned by hand, utilizing trial and error and a developed intuition for correcting the approximations. Two modeled results which were emulated in this way are shown in Figures 6 and 7.

Compounded Interference Observations

By considering combinations of the modeled radio science interference patterns from two meteoroid head-echoes, the majority of events analyzed here are likely emulated using two or more scatterers in the manner of Figures 6 and 7. Figure 8 shows some examples displaying both clear pulse-to-pulse cycling along with well defined intrapulse interference.

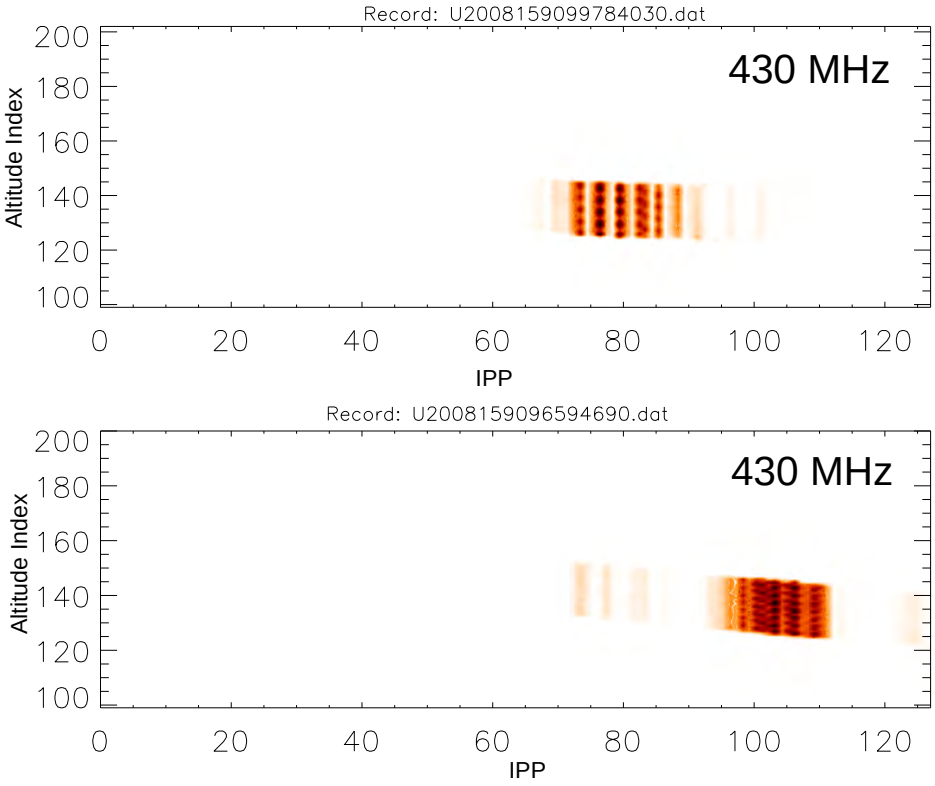

Figure 8: Two UHF RTI plots demonstrating the combination of a small number of fragments, greater than two, which created an interference pattern with clear pulse-to-pulse cycles in addition to intrapulse interference structures.

The intricate relationships between the interference created between each additional scatterer beyond the first interfering pair make the accurate emulation of such events nearly impossible to do by hand and brute force calculations except

for exceptionally simple events. More advanced processing techniques for finding the correct number of scatters and their properties, as shown in Roy *et al.*[7], while requiring greater computational power, would help affirm that these events are actually explained by fragmentation. The advanced processing techniques may even be helpful in determining the number and properties of scatterers of even more complicated events such as the nearly random appearing interference shown in Figure 9.

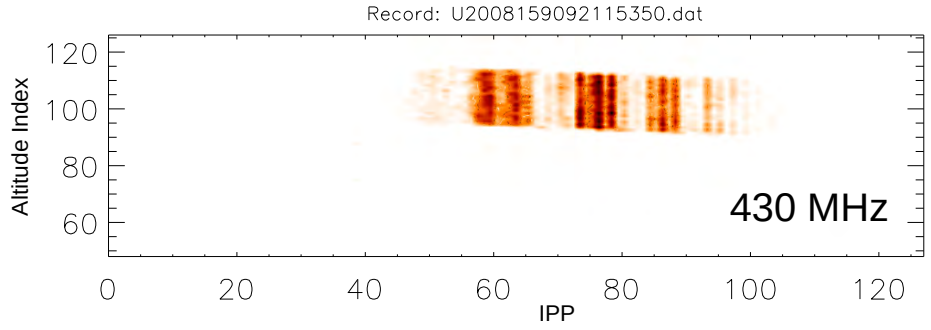

Figure 9: A UHF RTI plot demostrating the combination of a number of fragments of different speeds resulting irregular interference from numerous pulse-to-pulse cycling rates and intrapulse interference.

The event in Figure 10 at first appears to contain no interference patterns, regular or irregular. Closer inspection of that event's RTI plot (and those of many similar events) reveals that the near random noise within single pulses and from pulse-to-pulse is much greater than the background noise, suggesting that these events too are undergoing some amount of fragmentation. It may also be tempting to make the assumption that these radio science explanations are merely coincidentally flexible enough to explain the widely variable types of event specimens that were observed and to speculate that the interference cycling seen is instead the result of some combination of background noise, equipment error or other factors, such as ablation. While meteor science factors definitely play an important role in almost all of the observed events, a number of simultaneous, non-overlapping events suggest that the interference patterns cannot be attributed to radar system inaccuracies alone. Notice that in Figure 11, the lower event possesses noticeable pulse-to-pulse beating while the higher event possesses intrapulse interference along with some reflection of the UHF antenna gain.

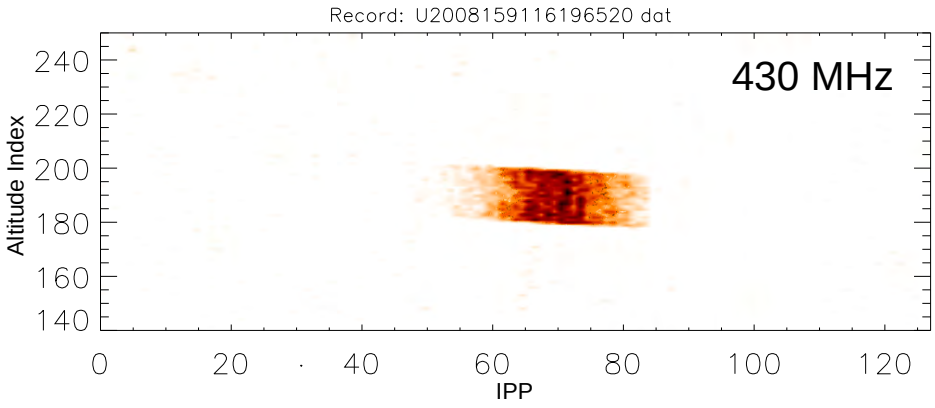

Figure 10: A UHF RTI plot, representative of a majority of meteor events analyzed, at first appears to be the smooth result of a single fragment passing through the main antenna lobe. Close inspection reveals intrapulse and pulse-to-pulse variations that have much greater variations than that seem due to background noise and is further inconsistent with the expected antenna gain. These variations could possibly be the result of interference created by the reflections of numerous small fragments around the larger scatterer that is dominant.

CONCLUSIONS

We have analyzed meteor events from Arecibo Observatory and found strong indications of signal interference and meteor fragmentation presence in nearly 100% of the observed events. We have successfully emulated some of these interference patterns using very simplified models of the involved radio science and helped to further verify the importance of meteor fragmentation.

Our demonstrated model may serve as a starting foundation for further simulations of micrometeors which include these radio signal interference properties. Further work could be incorporated into a 3D model while accounting for the antenna gain geometry. However, for now, the Arecibo Observatory does not possess the interferometric capacities that would contribute very important spatial information to complete these models accurately. Meteor science events, like ablation, as modeled by Dyrud and Janches[1] could also be integrated into a more robust model.

Additionally further investigation is warranted to explain a number of interesting meteor specimens, such as the possible existence of UHF trail-echoes, which have been highlighted by our classification of the Arecibo Observatory data.

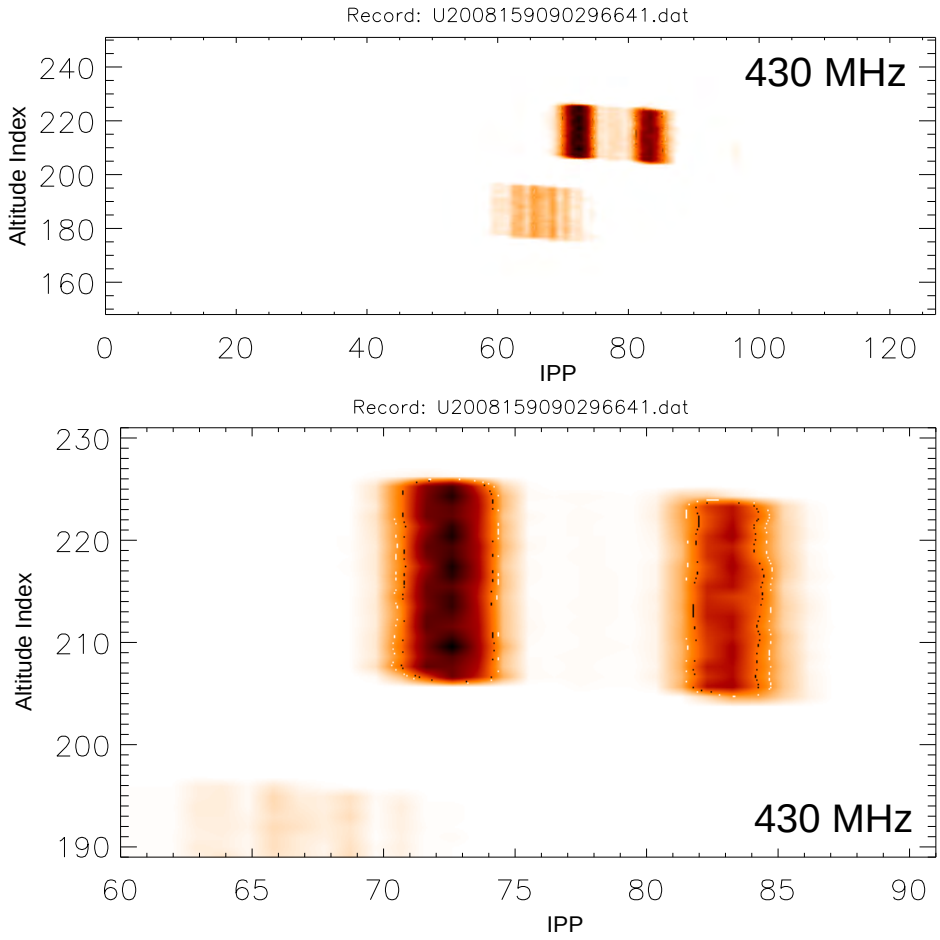

Figure 11: A UHF RTI plot that shows two simultaneous head-echoes, one possessing pulse-to-pulse cycling interference and one with intrapulse interference suggesting that these different interference patterns are not the product of equipment error alone.

ACKNOWLEDGEMENTS

This material is based upon work supported by the National Science Foundation under Grant No. EEC-0755081. The Arecibo Observatory is part of the National Astronomy and Ionosphere Center, which is operated by Cornell University under a cooperative agreement with the National Science Foundation.

REFERENCES

[1] L. Dyrud and D. Janches, "Modeling the meteor head echo using Arecibo radar observations," *Journal of Atmospheric and Solar-Terrestrial Physics*, **70** 1621–1632 (2008).

[2] M. I. Skolnik, *Radar Handbook*, 3 ed., McGraw-Hill Professional, New York, 2008.

[3] J. D. Mathews, S. Briczinski, D. D. Meisel and C. Heinselman, "Radio and Meteor Science Outcomes From Comparisons of Meteor Radar Observations at AMISR Poker Flat, Sondrestrom and Arecibo," *Earth Moon Planet*, **102** 365–372 (2008).

[4] J. D. Mathews, "Radio science issues surrounding HF/VHF/UHF radar meteor studies," *Journal of Atmospheric and Solar-Terrestial Physics*, **66** 285–299 (2004).

[5] J. Mathews, J. Doherty, C.-H. Wen, S. Briczinski, D. Janches and D. Meisel., "An update on UHF radar meteor observations and associated signal processing techniques at Arecibo Observatory," *Journal of Atmospheric and Solar-Terrestial Physics*, **65** 1139–1149 (2003).

[6] S. J. Briczinski, J. D. Mathews and D. D. Meisel, "Statistical and fragmentation properties of the micrometeoroid flux observed at Arecibo," *Journal of Atmospheric and Solar-Terrestial Physics*, **114** A04311 (2009).

[7] A. Roy, S. J. Briczinski, J. F. Doherty and J. D. Mathews, "Genetic-Algorithm-Based Parameter Estimation Technique for Fragmenting Radar Meteor Head Echoes," *IEEE Geoscience and Remote Sensing Letters*, **6** (3) 363–367 (2009).